FABRICATION AND PERFORMANCE TESTING OF A STEADY THERMOCAPILLARY PUMP WITH NO MOVING PARTS

Michael J. DeBar[1] and Dorian Liepmann[2]

[1]Eastman Kodak Company, Rochester, NY, 14650-2015, USA
[2]University of California at Berkeley, Berkeley, CA 94720, USA
Phone: (585) 477-3074, Fax: (585) 722-9053, Email: michael.debar@kodak.com

ABSTRACT

Pumping in microdevices due to gradients in surface tension was investigated experimentally. Devices exhibiting the Marangoni effect in square channels were designed and fabricated from one silicon substrate and one quartz substrate. The two substrates were aligned, bonded and packaged for testing. Each of the devices consisted of a 100μm channel with three heaters along one of its sides. One heater generated a fluid-vapor interface while another controlled the temperature gradient along this interface. Flow could be generated in either direction, and could be switched on and off nearly instantaneously. Pressure was measured during device operation, and flow rate was measured indirectly through its proportionality to the time derivative of pressure in a quasi-steady flow.

The devices were operated at a variety of heater settings to evaluate their performance over a range of flow rates and pressures. A minimum energy of 140 mW was required from the central heater to generate and maintain the vapor bubble, and the flow rate increased with input energy. The efficiency of the device increased with flow rate, since the overhead to create and maintain the bubble (140 mW) dwarfs the energy expended to generate the temperature gradient (15-50 mW). The devices generated a maximum pressure head of 44 Pa, and a maximum flow rate of 9.3 nL/s, although the maximum values did not occur simultaneously. In fact, the maximum pressure will always occur when the flow rate is zero, and vice versa.

INTRODUCTION

When a gradient in surface tension exists along an interface between two fluids, there is a net motion of the interface, referred to as the Marangoni effect. This induces a flow parallel to the interface through viscous diffusion. In microdevices, where length scales are very short, this can drive fluid flow at significant flow rates due to the dominance of surface tension in this regime [1]. This provides a mechanism for steady pumping in microscale devices, without the use of moving parts. When a vapor bubble is created, and a temperature gradient is imposed, the resulting surface tension gradient will drive the flow from the hotter side of the vapor bubble to the cooler side.

FABRICATION

The fabrication of the bubble pump consists of several different processes. First, channels and reservoirs are etched into the silicon wafer, while heaters are deposited onto the quartz wafer. This can be done in parallel, as the processes are independent. Once both halves of the device are complete, the wafers are diced, and bonded on a die-to-die basis. A fabrication chart for both the silicon and quartz wafers is shown in Figure 1. Finally, the completed microdevices are removed from the cleanroom environment, and packaged for connection to testing equipment in the macro world.[2]

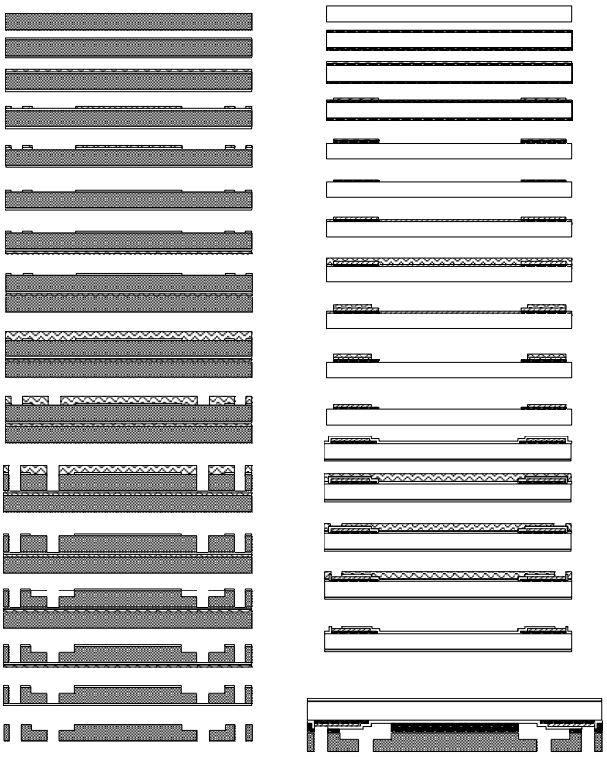

Figure 1: Fabrication chart showing die fabrication. A silicon die is on the left, and the quartz is on the right. At the bottom is an enlarged bonded device.

Fabrication of the reservoirs, channels, and through holes in the silicon wafers is straightforward. Two masks are over-

laid onto the silicon, and a two-level silicon etch completes the devices.

The quartz wafer is coated with n-doped LPCVD polysilicon, annealed, and then patterned and wet etched in silicon etchant. The pattern for the polysilicon layer included both the heaters themselves, and the traces and pads where the aluminum will be deposited. Subsequently, aluminum (2% Si) is sputtered, then patterned. Finally, silicon dioxide is deposited via low-temperature LPCVD and patterned to expose the electrical contacts. An additional benefit of this process is an annealing of the aluminum layer to the polysilicon along the traces and pads.

EPO-TEK 301 is spin-coated onto the quartz die, since it has less topography. Dies are aligned and pressed together manually by looking through the quartz wafer. The alignment is checked on a light microscope, and fine corrections are made. This gives an accuracy of better than 5 μm alignment (comparable to 5 μm accuracy in previous work on a flipchip bonder). Excess epoxy is then removed by subjecting the bonded devices to an oxygen plasma until channels are clear.

Each device is then mounted, quartz-side down, over an 8mm viewing window in an externally manufactured circuit board and electrical connections are wire-bonded. Once the connections are resistance tested (resistances range from 1.7-1.9 KΩ), modular fluidic connections are epoxied to the device. The circuit board then interfaces with an edge board connector, and then interfaces with a breadboard for easy access to all leads, and Luer-Lock connectors allow the device to be easily inserted into a fixed setup for testing.

TESTING

Once the chips were packaged, multiple heaters were powered with separate power supplies. Voltage was controlled by adjusting the output of the power supplies. A switch could be toggled to direct power from one gradient-generating heater to the other, reversing the direction of induced flow. This was demonstrated experimentally by using constant voltage on the central heater, and a variable voltage on the gradient-generating heater.

When the heater was pulsed, flow was induced from the heated side to the unheated side. The delay between activation and motion was momentary. When the switch was flipped and the other heater was activated, flow direction reversed. Fluorescein-coated particles seeded the flow for easy visualization.

During all of the experiments, the bubble interface fluctuated and moved from side to side. Speeds within and near the bubble were very high, at least an order of magnitude higher than the fluid flow upstream and downstream of the bubble. A recirculating flow, due to the mass transfer of the boiling process, existed within the bubble. The system was

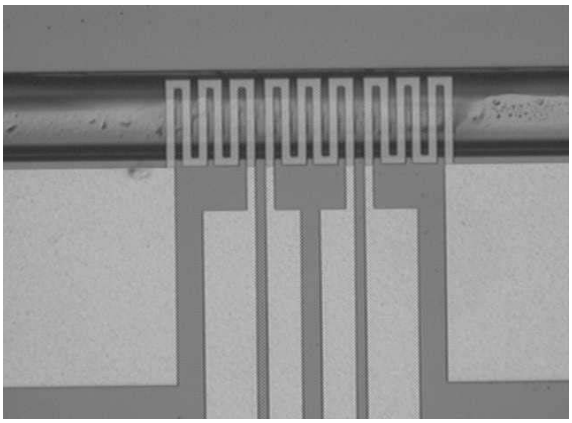

Figure 2: Top view of a fabricated Marangoni pump. Channel cross-section is 100μm square.

not in a steady state. Although there was a net flow is one direction, the flow "stuttered", and backflowed at times. This effect became more obvious when numerical data were examined, but it was evident during qualitative experiments, especially during longer runs. The flow could occur in either direction, and sometimes varied from run to run. This appears to be some sort of instability in the system, but it can be overcome by imposing a temperature gradient. Flow could be driven in either direction, based on the temperature gradient imposed by the gradient-generating heater. In general, a voltage of 15 volts was used on the central heater, while a voltage of 7 volts was used on the gradient-generating heater. Excessive voltage on the central heater resulted in heater burnout, and a loss of the use of the heater in future experiments. This is the primary failure mode of the devices at this time. It is most common when the device reaches an equilibrium state, where the net flow rate is zero while the device is pumping. Under these conditions, the heat in the region near the heater can build up, and there is no convection to dissipate the heat.

Overall, the use of two heaters provided control of flow speed and direction. A single heater could generate a bubble and some flow based on the temperature gradients within the bubble, but the second heater provided control of the temperature gradient, and therefore the flow speed and direction. Additionally, this reduced wasted energy due to internal recirculation.

Subsequently, pressure was measured as a function of time in a powered device. The device was hooked into the bottom of a U-shaped system. The excess pressure on the pumping side was recorded for 4 minute periods. One run is shown in Figure 3.

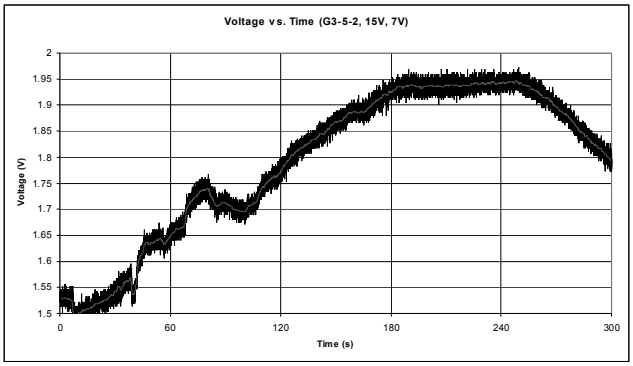

Figure 3: Pressure data for device G3-5-2 (15V, 7V)

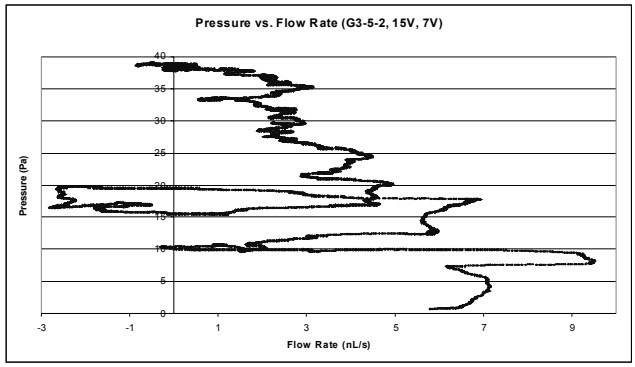

Figure 4: Pressure vs. flow rate for device G3-5-2 (15V, 7V)

When the device was powered, the pump began pumping toward the side with the pressure sensor (by design), using two heaters at constant voltages. Prior to each run, the pressure was sampled at 100Hz for five minutes, until there was no appreciable variation in the signal, other than the inherent noise due to the high gain used for all experiments. Typically, the equilibration took about 10 minutes between runs, depending on the amount of fluid pumped in the previous run. Data was taken at a variety of input voltages, and maximum pressures and flow rates are shown in the table below. These values did not occur simultaneously.

RESULTS

The data recorded during pumping not only contain the pressure as a function of time, but also the flow rate. In order to extract these data, the slope of the curve must be determined. For a constant density, gravitational field, and cross-sectional area, conservation of mass dictates that:

$$Q = AU = A\frac{dh}{dt} = \left(\frac{A}{\rho g}\right)\frac{dP}{dt}$$

where the change in height is converted into a change in hydrostatic pressure. The raw data show, however, that the slope is constantly reversing sign due to the noise of the signal. The average noise is about 20mV for a signal of 1.0-2.0 volts. In order to eliminate this noise, each data point is replaced by a 101-point moving average, representing the one second of data surrounding the point. The slope is calculated based on this average. This is still very noisy, however, so the slope is calculated across 1000 points (10 seconds). This is then scaled and graphed against the pressure, and is shown in Figure 4 for the data set corresponding to Figure 3. The data after equilibration were removed for samples that equilibrated.

There are a number of interesting features present in the graphs. The pressure increases at a decreasing rate as fluid is driven into the column containing the pressure sensor. As the column height rises, a greater and greater force resists the pump's effects, and the flow rate decreases. This results in a monotonically increasing but concave downward pressure versus time graph whose asymptote is the maximum attainable pressure for the device, at those particular power inputs. If the pressure versus flow rate graph is constrained to be linear, then pressure must be proportional to its own derivative, indicating an exponential function of the form

$$P(t) = P_{max} - Be^{-Ct}$$

where both B and C are positive numbers. The graph in Figure 3 shows this type of behavior. After 250 seconds, however, there is a decrease in the pressure. This is the result of a burned-out heater. After reaching a region of no flow, heat built up and caused failure of the bubble generator. With the collapse of the bubble, the fluid began to backflow to the zero pressure baseline. The other interesting feature in this graph is the overshoot and correction behavior seen between 50 and 100 seconds into the test. These changes are due to the instabilities in the system, as discussed in Section 5.3. These swings are magnified when the derivative of the graph is considered. Due to corrections like these, the pressure versus flow rate graphs magnify the instabilities present in the system, but there is still a linear trend in the data, especially for higher pressures.

When the main heater voltage was reduced to 13 volts, a different type of flow developed. The pressure in this case increased very slowly and then began to increase faster. Qualitative observations made previously indicate that this behavior is due to the inability of 13 volts to form and maintain a uniform bubble. The temperature near the bubble slowly builds, gradually increasing the pressure gener-

ated by the pump. The flow rate in this case actually increases with pressure.

The generating heater was returned to its starting value of 15 volts, and the gradient-generating heater was varied from its 7 volt starting point. The other graphs show similar behavior to Figure 3, except that the runs generally take longer to reach an equilibrium value when the voltage is below 7 volts.

The 8-volt sample contained another interesting feature. The pump alternated between two nearly constant flow rates, changing from one behavior to another quite suddenly. This behavior was attributed to an instability in the system, but the nature of the instability has not yet been determined. The flow rate oscillated between 1 nL/s and 5-7 nL/s as the pressure increased.

The maximum pressure reached at equilibrium is a good measure of the effect of gradient-generator voltage. Higher voltages generated more pressure, except for the case of the 6-volt run. In addition, the maximum pressure reached in the 13-volt bubble generator case was just over half of the value reached in the 15-volt case. The maximum flow rate was also a barometer of performance, albeit one with a greater uncertainty. Once again, a general trend of higher flow rates for higher input energy was confirmed, but this parameter was not as conclusive as the maximum pressure..

Table 1: Maximum Pressures and Flow Rates for Various Voltage Settings (G3-5-2)

Bubble Generator Voltage	Gradient Generator Voltage	Maximum Pressure	Maximum Flow Rate
15.0V	7.0V	39 Pa	9.3 nL/s
13.0V	7.0V	25 Pa	2.1 nL/s
15.0V	5.0V	21 Pa	2.7 nL/s
15.0V	6.0V	39 Pa	3.7 nL/s
15.0V	8.0V	44 Pa	7.5 nL/s

From these results, it is evident that the bulk of the input power generated and maintained the bubble, and only a small portion of the energy caused fluid motion. This small amount above and beyond the baseline required to generate fluid motion had a substantial effect, however. A reduction of the bubble generator voltage to 13 volts reduced the device efficiency by an order of magnitude. Reducing the heat to the gradient-generating heaters was also inefficient. Once the threshold value for motion has been reached, the return on power investment was significant; a slight increase in the gradient-generating heater had appreciable effects on the efficiency. The high pressure seen in the 6 volt sample is less of an anomaly by this data, since its efficiency is poor. Although a high pressure head was generated, the low flow rate accompanying it could not measure up to the most efficient case at 15 volts and 7 volts.

CONCLUSION

A novel pump design based on the Marangoni effect was fabricated and tested. The pump is comprised of 4 key elements: a square channel, a bubble generating heater, and 2 thermal gradient generating heaters. When a bubble is created by the bubble generating heater within the square channel and a thermal gradient is created by one of the gradient generating heaters, fluid flows from the hotter region of the liquid-vapor interface to the cooler region. Flow continues until the temperature gradient is removed.

Pumping in both directions was demonstrated. As the device pumped fluid into one side of the U-tube manometer, the hydrostatic pressure working against the pump increased and the flow rate of the pump, measured from the change in height of the column, decreased until the device reached a maximum pumping pressure at zero flow rate. When the bubble generating heater provided less than 140 mW, the heater could not create and maintain a single bubble. The gradient generating heater power was also tested; flow rate was shown to increase with the power supplied to the gradient generating heater for equal bubble generator voltages. The maximum pressure generated during any run was 44 Pa, and the maximum flow rate (from a diferent run) was 9.3 nL/s. There are many other modifications that can be made for specific applications, including making arrays of devices to increase the total pressure head and flow rate, adjusting resistor values to optimize the range of flow rates for a given voltage, and assembling fluid sorting devices. The pump is extremely versatile and easy to fabricate, and would be a valuable component in numerous integrated microfluidic systems.

ACKNOWLEDGMENTS

This work was supported by DARPA and the Eastman Kodak Company.

REFERENCES

[1] N.O. Young, J.S. Goldstein, M.J. Block, “The motion of bubbles in a vertical temperature gradient.” JFM 6, 1959.

[2] M. DeBar, “Control of Fluids in Microscale Devices.” Ph.D. Thesis, UC Berkeley, 2001.

[3] J. Evans, D. Liepmann, and A.P. Pisano, “Planar Laminar Mixer.” MEMS ‘97.